ESTIMATION OF UNCERTAIN MATERIAL PARAMETERS USING MODAL TEST DATA*†

Paul S. Veers‡
Daniel L. Laird‡
Thomas G. Carne§
Mathias J. Sagartz§
Sandia National Laboratories
Albuquerque, New Mexico 87185
USA

Abstract

Analytical models of wind turbine blades have many uncertainties, particularly with composite construction where material properties and cross-sectional dimension may not be known or precisely controllable. In this paper we demonstrate how modal testing can be used to estimate important material parameters and to update and improve a finite-element (FE) model of a prototype wind turbine blade. An example prototype blade is used here to demonstrate how model parameters can be identified. The starting point is an FE model of the blade, using best estimates for the material constants. Frequencies of the lowest fourteen modes are used as the basis for comparisons between model predictions and test data. Natural frequencies and mode shapes calculated with the FE model are used in an optimal test design code to select instrumentation (accelerometer) and excitation locations that capture all the desired mode shapes. The FE model is also used to calculate sensitivities of the modal frequencies to each of the uncertain material parameters. These parameters are "estimated," or updated, using a weighted least-squares technique to minimize the difference between test frequencies and predicted results. Updated material properties are determined for axial, transverse, and shear moduli in two separate regions of the blade cross section: in the central box, and in the leading and trailing panels. Static FE analyses are then conducted with the updated material parameters to determine changes in effective beam stiffness and buckling loads.

Introduction

Wind turbine blades need to be analyzed to evaluate a number of design constraints. The ultimate strength needs to be sufficient for extreme loads; buckling-stability analyses are required for any unsupported panels; a detailed stress analysis is needed before reasonable fatigue life assessments can be made; and elastic characteristics of the blade as a whole must be determined for inclusion in system dynamic models such as ADAMS-WT[1], FAST[2], or BLADED[3]. Without accurate structural and material properties for the blade, the calculation of blade stresses and turbine response will produce inaccurate results and a greater probability of prototype failure. It is also our intent to use the procedure described here to evaluate the materials produced in future manufacturing research efforts.

There are many reasons that blade structural properties may be difficult to determine. Most blades are made of composite materials, which are inherently more variable than homogeneous structural materials such as metals. Most are manufactured by hand lay-up methods that increase their variability from design specification. Wood laminates are also used in some applications. The properties of the wood are sometimes variable from laminate to laminate. Even pultrusions, which have the benefit of automation and continuous processing, can have uncertain material properties because changes in the fiber or resin content may be

* This work is supported by the U.S. Department of Energy under Contract DE-AC04-04AL85000 and DE-AC36-83CH10093. Sandia is a multiprogram laboratory operated by Sandia Corporation, a Lockheed Martin company, for the U.S. Department of Energy.
† This paper is declared a work of the U.S. Government and is not subject to copyright protection in the United States.
‡ Wind Energy Technology Department
§ Experimental Structural Dynamics Department

made in the final stages of production for manufacturing reasons.

Simple tests can be used to measure effective beam stiffness (flexural rigidity, EI) directly from load deflection results. Although effective beam properties may be determined from static testing, detailed information on material properties at different locations within the blade can not be determined from such simple tests. And, it is often necessary to determine blade material properties locally, as well as averaged over the cross section, because detailed stress analysis and panel-buckling stability can depend on differences in material properties within a single cross section.

A method that combines analysis and test results to determine blade material properties within the cross section is illustrated here. Finite-element (FE) analysis is used to calculate blade mode shapes and frequencies and to estimate the sensitivity of each modal frequency to parameters of interest; e.g., material properties. Modal testing is used to measure the frequencies and mode shapes of a blade. The higher modes, because of their more complex shapes, strain parts of the blade cross section in different proportions and directions, making the modal frequencies sensitive to the cross-sectional properties by different amounts. Thus, the higher modes give us insight into the material properties at different locations and in different directions within the blade cross section. The analytical sensitivities are used to drive a MatLab© software shell called PESTDY[4] (Parameter EStimation for STructural DYnamics). It calculates a weighted least-squares estimate of the material properties that best bring the analysis frequencies into alignment with the test frequencies. PESTDY has been used on many other systems and was not developed specifically for the wind-turbine blade application. Finite element analyses can use the updated material properties to determine effective beam-bending properties, static stress distribution, and buckling strength.

Wind Turbine Blade Example

It is useful to conduct an actual parameter estimation with a real wind turbine blade to illustrate the procedure and to show typical results of a material property updating exercise. A prototype blade segment from a FloWind wind turbine was available for use. This constant 0.69m chord 0.122m thick blade was designated the “B-blade” to distinguish it from the initial design “A-blade” and the final design “C-blade.” The B-blade is therefore not the final blade used on the FloWind prototype.

The FloWind blades are pultruded, glass-fiber reinforced plastic blades. The initial test section was a 5m long constant-chord section of the much longer (approximately 55m long) blade. The B-blade cross section, as measured for the parameter estimation exercise, is shown in Figure 1. The blade cross section is divided into two regions with material properties assumed to be different between each region but uniform within each region and constant along the blade span. The two regions are the central “box” and the “panel” sections both fore and aft of the central box. Figure 2 shows the box section dark and the panels light. All the panels are assumed to have similar properties because the manufacturing process uses large fabric sheets that wrap most of the way around the airfoil section, comprising most of the material in all the panels. The skin portion of the box section contains additional reinforcement, while the two ribs are made of similar fabric types, but with smaller sheets. Some fabric sheets wrap around the corner, connecting the ribs to the skin. The assumption of uniform properties within the box is less accurate than in the panels. One elastic modulus is assumed in each principal direction (axial and transverse) and one shear modulus is assumed in each region of the cross section. Original

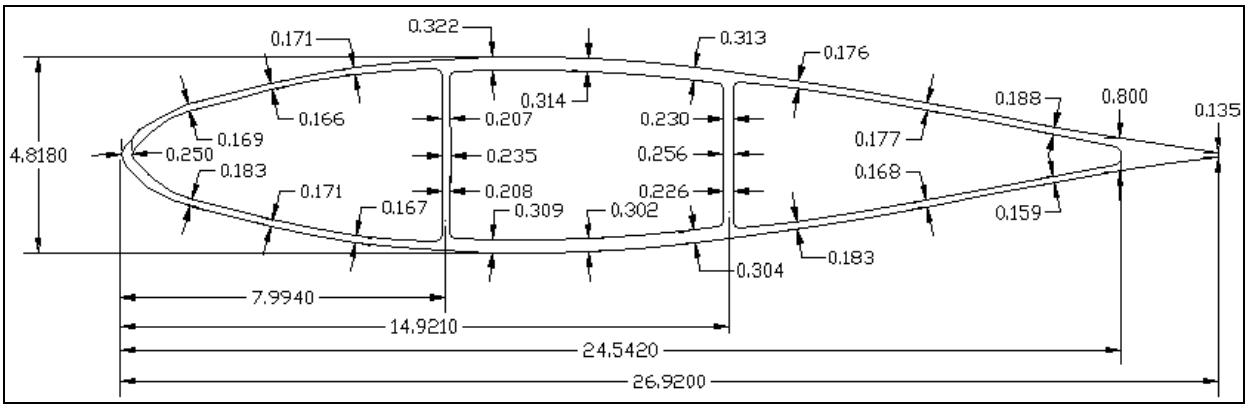

Figure 1. Cross section of the B-blade. All dimensions are in inches.

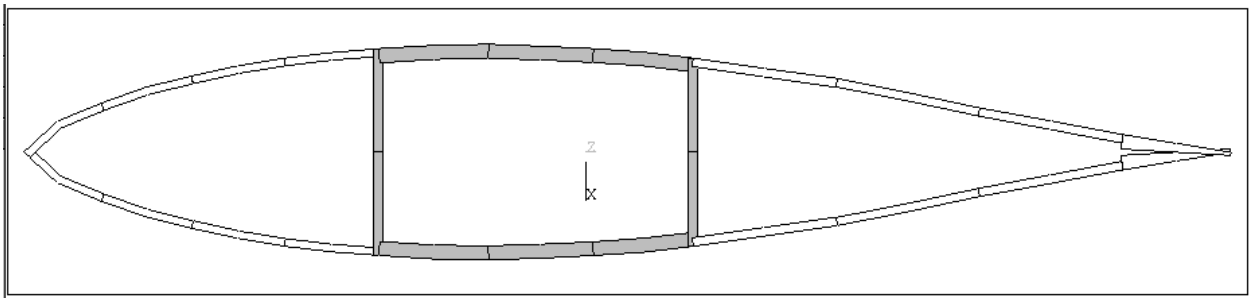

Figure 2. Cross-sectional view of the original FE model. Though shell elements were used, this representation shows the thickness values associated with each element. The dark shading indicates the "box" region and the light shading is the "panel" region.

Cross Section Region	Material Modulus Direction		
	Axial	Transverse	Shear
Box	5.0	1.0	0.6
Panel	5.0	1.5	1.0

Table 1: Initial Material Properties (in 10^6 psi)

material properties, shown in Table 1, are not based on industry-supplied estimates, but are rough, round-number starting points for illustration purposes only.

This division of material properties into two sections is an obvious oversimplification. It is, however, a huge improvement over treating the entire cross section as a single material and it divides the blade into two regions that could have different material properties because of differing lay-ups. The number of unknowns should be less than the number of measurements for a least-squares type parameter estimation to be used here. With 14 measured frequencies, a reasonable limit for the number of unknowns is six to eight. Therefore, dividing the cross section into two regions and estimating three material properties in each region is a reasonable compromise for the amount of test data available.

The 5m B-blade test piece was originally intended for resonant fatigue testing. For these tests, the blade was subjected to modal testing to determine the best locations for load attachment and support points. An initial attempt at material parameter estimation was done with modal test data from the 5m test piece. A simple ANSYS[5] shell analysis was done and parameter estimation conducted, just as described below. However, because the modal test was done only for the purpose of fatigue test planning, the goal was to establish only the first mode and frequency and not to characterize the more complex mode shapes. Matching the higher modes between test and analysis was subject to some uncertainty. This initial parameter estimation exercise was therefore judged inadequate to demonstrate the process. The fatigue test ultimately damaged only one end of the 5m blade segment, leaving 4m for additional testing. It was therefore decided to cut off the broken portion of the blade and redo the parameter estimation using a better analytical model and a modal test aimed specifically at the parameter estimation objective. The following describes the blade finite element analysis, test planning, modal test, and parameter estimation procedure of this second round of analysis and test.

Results from the first round of parameter estimation (on the 5m blade segment) are included as well.

Finite-Element Analysis

The FE analyses utilized three different models. The first, "Original," model corresponds to the original blade segment length of 5m (192 inches). The "Interim Model" simply chopped 1m worth of elements off the original to match the shortened blade and provided information used in selecting locations for the placement of accelerometers in the experimental design. And finally, a more refined model, called the "Current Model," was generated in an attempt to best match the experimental results.

Original Model

The original blade, 5m (192 inch) length, was first analyzed for the purpose of planning the fatigue test. The FE analysis used eight-node isoparametric shell elements with six degrees of freedom (dof) at each node. The model contained 390 elements and 1160 nodes resulting in 6960 dof. This model is shown in Figure 3. The blade geometry was assumed to be ideally symmetric. Skin and rib thickness values were assumed to be identical from one side of the blade to the other. The tail portion of the blade was modeled as two shell areas connected at a single line of nodes along the trailing edge. Figure 2 shows a cross-sectional view of the model. The thickness values assigned to each element are represented in this view. This model was used in the initial parameter estimation exercise.

Interim Model

The first attempt to analyze the shortened blade of 4m (154 inches) utilized the original model with some of the elements deleted. All features and limitations of the original model were unchanged. The material properties used for the shortened model corresponded to the optimized properties from the initial parameter estimation exercise. This model was used to guide the placement of accelerometers for the modal test described below.

Figure 3. Finite element shell model of original blade (5m, (192 inch) length). The model has 6960 degrees of freedom.

Current Model

In the development of the current model, efforts were taken to improve the accuracy by reducing the number of modeling assumptions and by increasing the mesh density. In addition, the blade weight and cross section measurements were used to calculate the material density, which was found to be almost 9% higher than originally thought. This higher density was used in the current model.

No assumptions were made as to symmetry of skin thicknesses or rib thicknesses. While Figure 1 gives the rough description of the section, the actual data used included over 40 measurements of wall thicknesses in both the skin and the support ribs at one cross-section location. Next, an entirely new model was created with a greater number of elements used in the cross-section and in the axial direction of the blade. The entire model is shown in Figure 4 while Figure 5 shows the cross-section. Again, eight-node isoparametric shell elements are used but the mesh density in the axial direction of the blade is three times that of the original model. As shown in Figure 5, over twice as many elements are defined throughout the cross section and the varying wall thicknesses are incorporated into the model. Each different thickness is given a different shading.

As indicated in Figure 1, the trailing edge is in fact solid. While the original model did not account for the solid tail section, the current model includes two narrow ribs to approximate the transverse stiffness of the solid tail without adding to the overall mass or the axial stiffness.

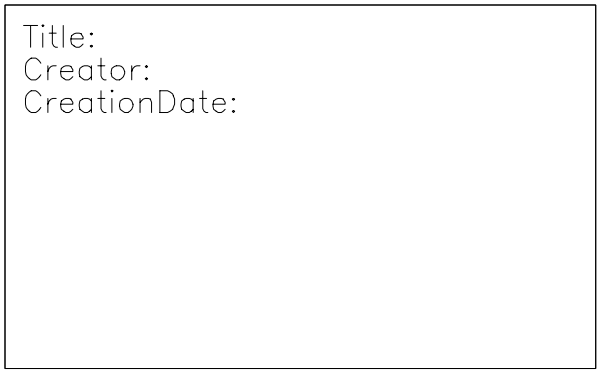

Figure 4. Finite element shell model of current blade (4m, 154 inch length). The model has 41,000 degrees of freedom.

Analysis Results

After results of the interim model were used to guide the experimental set-up, the current model was developed and used for all subsequent analyses. The results of a modal analysis and estimates of the sensitivities of the frequencies to the material parameters were then used to estimate the parameters.

Interim Model

The natural frequencies resulting from the modal analysis are shown in the second column of Table 2. The first 13 flatwise natural frequencies plus the first edgewise frequency (which is significantly higher) are listed. Names were assigned to each mode based on the mode shape and using a plate-mode naming convention where appropriate (shown in the table in parentheses). The number of nodal lines parallel to the chord line is given first, followed by the number of nodal lines parallel to the blade span. The material properties used for this analysis were the optimized material properties from the first study, called the interim properties, and are given in the third column of Table 3.

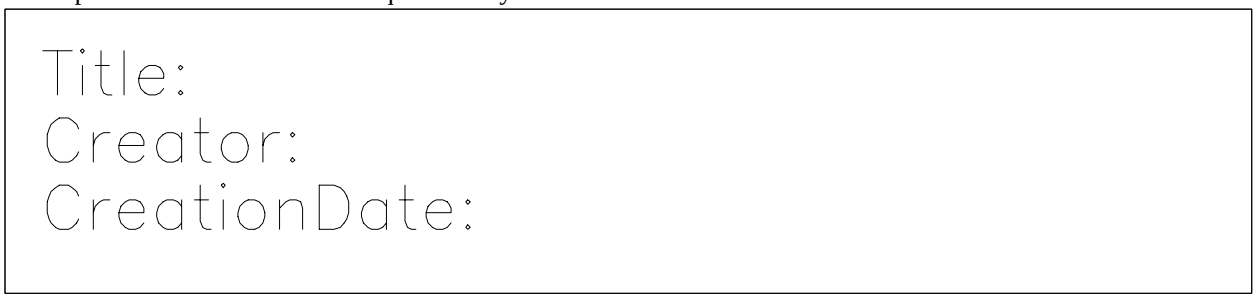

Figure 5. Cross-sectional view of current model. Though shell elements were used, this representation shows the thickness values associated with each element.

Current Model

The current model was used to perform a modal analysis. The resulting natural frequencies are given in Table 2. Figures 6 and 7 show the first and seventh mode shapes, respectively, from the analysis. The material properties used were the same ones used in the interim model (interim properties), except for the increase in material density by 9% based on measurements. The panel frequencies are all higher than the associated frequencies from the interim model. This indicates that the interim model was probably too soft and that the material parameters optimized for that model were probably too stiff. The modeling error can be traced to a single point connection between the top and bottom panels along the trailing edge, which was too soft of a tail connection and led to falsely high estimates of the transverse panel modulus.

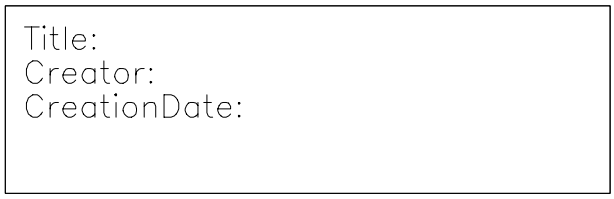

Figure 6. First bending mode. Contours indicate relative displacement.

Figure 7. Seventh mode (106 Hz) with contours indicating relative displacement.

FE Model	Interim Model	Test	Current model

Material Property set	Interim (initial density)			Interim (higher density)		Final	
Mode Number - Name	Hz	%	Hz	Hz	%	Hz	%
1 - 1st Flatwise (2-0)	37.478	-1.00	37.857	38.1	+0.6	37.579	-0.734
2 - 1st Twist (1-1)	68.442	+4.40	65.557	63.8	-2.6	63.705	-2.83
3 - 2nd Flatwise (3-0)	80.052	+2.93	77.777	83.0	+6.7	79.443	+2.14
4 - 2nd Twist (2-1)	88.760	+3.58	85.696	88.9	+3.7	85.234	-0.539
5 - 1st Chordwise (0-2)	95.374	+7.62	103.24	97.2	-5.8	97.805	-5.26
6 - 3rd Panel	103.04	+8.31	95.135	104.3	+9.6	100.04	-4.90
7 - 2nd Chord/1st Twist (1-2)	103.45	-7.49	111.83	112.4	+0.5	106.35	-4.90
8 - 3rd Twist (3-1)	108.23	-9.17	119.163	117.0	-1.8	109.99	-7.70
9 - 2nd Chordwise (0-3)	111.29	----	----	117.6	----	110.76	----
10 - 4th Panel/3rd Twist	111.36	+2.83	108.29	119.6	+10.3	114.26	+5.51
11 - 4th Twist (2-2)	120.31	-6.30	131.15	127.2	-3.0	121.24	-7.56
12 - 5th Panel	122.77	+0.87	121.71	132.0	+8.5	124.71	2.46
13 - 6th Panel	123.48	-8.25	134.59	144.2	+7.2	136.45	1.38
14 - 1st Edgewise	163.27	+4.83	155.75	156.6	+0.5	155.45	-0.193

Table 2. Natural Frequencies from the modal test compared with analytical estimates with different material property sets.

Material Property Set	Original	Interim		Final		
Cross Section Location	10^6 psi	10^6 psi	Change %	10^6 psi	Increment %	Total Change %
Box axial	5.00	4.213	-15.7	4.044	-4.0	-19.1
Box transverse	1.00	1.027	+2.7	1.281	+24.7	+28.1
Box shear	0.60	0.651	+8.5	0.724	+11.2	+20.7
Panel axial	5.00	5.027	+0.5	5.027	+0.0	+0.5
Panel transverse	1.50	1.871	+24.7	1.424	-23.9	-5.1
Panel shear	1.00	0.867	-13.3	0.859	-0.9	-14.1

Table 3. Material Property Estimates

Modal Testing

A modal test consist or three elements: (1) test design, (2) measurement of the frequency response functions (FRFs) between input locations and response locations, and (3) extraction of the modal data from the FRFs. Each of these will be discussed in this section along with a comparison with predictions from the original FE model.

Test Design

Modal testing requires a large number of expensive sensors, sophisticated analysis software and careful fixturing of the test piece. Careful design is critically important to insure that the data are useful for the ultimate purpose of understanding the structure and validating numerical models. We usually attempt to support the blade with free boundary conditions. Free conditions are very easily simulated in an FE analysis and fairly easy to approximate in the lab. Fixed boundary conditions, on the other hand, are simple to analyze, but virtually impossible to simulate perfectly with test fixturing. It is important to not introduce significant uncertainty into the test/model comparison by using uncertain boundary conditions.

As part of the test design, an FE model of the blade was created (the interim model) to compute the modal frequencies and shapes. Using this preliminary analysis as an aid in the design, we decided to measure all the modes to 150 Hz (fourteen modes in the analysis) which included flatwise bending, twisting, panel, and edgewise bending modes. These modes provide an information intensive set of data, including mode shapes that strain different parts of the cross section in different directions. Shakers were chosen as the primary excitation device, in contrast to hammer impact or step-relaxation, because the blade was relatively highly damped. Experience has shown that

shakers would be able to best excite the modes. Light-weight Kistler© 8639B50 accelerometers were used as transducers to minimize the added mass, which could influence the results. Testing was performed in a high-bay laboratory using an overhead crane to suspend the blade with long bungee chords and nylon slings to approximate free boundary conditions. As shown in Figure 8, the blade was suspended with the chord in the vertical plane and the leading edge down. The pendulum frequency, due to the support conditions, was 0.24 Hz which was far enough from the first frequency to have negligible effect on the flatwise modes. The vertical "rigid-body" bounce mode on the bungee chords was 1.1 Hz, which will not affect the edgewise mode.

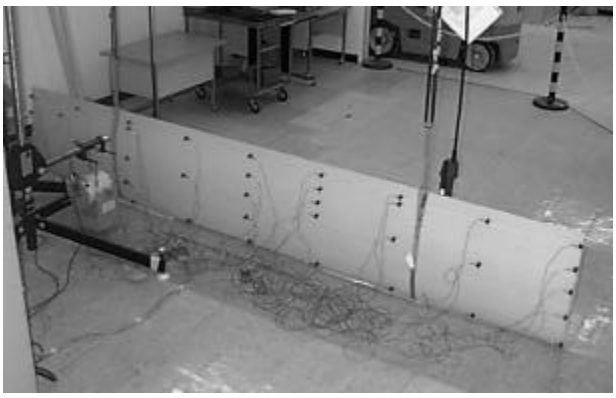

Figure 8: Blade test setup with bungee suspension, wiring, accelerometers and shaker.

One requirement of a modal test design is to chose measurement locations and directions so that one can identify the various mode shapes.[6] A minimum number of transducers reduce the cost and complexity of the test. However, there are two design requirements on selection of transducer locations; enough locations must be chosen so that the data can be used to visualize the deformation of the modes and to obtain correspondence between the test-based modes and the model-based modes. Correspondence is obtained through the use of the Modal Assurance Criterion (MAC).[7] The equation for the matrix of MACs is

$$\mathrm{MAC}_{ij} = \mathrm{MAC}(f_i, f_j) = \frac{(f_i^T f_j)^2}{(f_i^T f_i)(f_j^T f_j)}, \qquad (1)$$

where f_i is the mode-shape vector of the ith mode. Each element of the MAC matrix, MAC_{ij}, is the normalized dot product squared between the vector shapes i and j. It reveals how similar the two mode shapes are, with numerical values varying between zero and one. (1.0 indicates perfect correlation.) MACs can be calculated between the test-based and the model-based mode shapes to determine match-ups between test and analysis modes. In the test design, MACs are calculated between the analytical mode shapes using f_i values at candidate accelerometer locations. Consequently, one must choose transducer locations so that the off-diagonal MACs are low for all the modes of interest, assuring that the modes of interest can be distinguished from one another using data from the proposed locations. This procedure has been automated in a code, Optimal Test Design[6] (OTD). OTD uses the mode shapes obtained from the preliminary FE model of the structure. One selects an "intuition" set of locations from the nodes of the FE model to assure visualization of the shapes, and then OTD suggests additional locations, which are added until the off-diagonal MACs are sufficiently low.

A set of thirty-nine locations were interactively selected using OTD. An interactive MatLab© script was written to automate and simplify the process of transducer location selection. The user inputs either a list of node numbers from the FE analysis or selects transducer locations interactively by clicking on a location inside a blade outline. If the user inputs a list of node numbers, their coordinates are displayed on the blade outline. Additional locations can be selected by clicking within a blade outline. Although thirty-nine is a fairly small set of transducer locations, reducing the cost of the test, these locations are sufficient to both visualize the shapes and obtain correspondence with the analytical mode shapes. Figure 9 shows an outline of the blade with the selected locations. All transducers are uniaxial, measuring flatwise motion, except for five biaxial transducers which are included to also measure edgewise motion.

Another aspect of the modal test design is determining the location, direction, and number of excitation points that will significantly excite all the modes of interest. Most frequently, multiple locations are required in order to excite all the modes. Excitation design can also be performed within the OTD code, again based on the preliminary FE model. The input to OTD includes the model-based mode shapes and modal frequencies, so frequency response functions (FRFs) due to a particular force input can be computed analytically and evaluated for excitation candidates. OTD uses the Mode Indicator Function (MIF)[8] to determine whether a mode is sufficiently excited. Several candidate excitation locations are evaluated with the MIF; one or more are selected depending on how many inputs are required to excite all the modes.

For this blade segment, we need three inputs to sufficiently excite all the modes. The first two were in the flatwise direction at nodes 7811 and 8292, and the third was on the leading edge at the center of the blade in the edgewise direction.

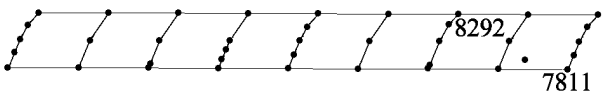

Figure 9. Diagram of blade with the measurement node locations. The leading edge is up.

Measurement of FRFs

The FRFs were measured using multiple simultaneous inputs, collecting all the thirty-nine response functions for the two flatwise inputs in one testing session. The shakers were driven with burst random signals where the signals were filtered to remove frequencies above 200 Hz. The data window was ten seconds in duration and the pulse duration was limited to eighty percent of the window, so that the response would damp to zero by the end of the sampling window. FRFs were measured using twenty samples. The driving point FRFs for the two input locations are shown in Figure 10. Notice that the inputs compliment each other, one providing good excitation of some modes that are not excited by the other. For example, there are two modes near 120 Hz. The input at 7811 excites the higher mode quite well, but not the lower, while the input at 8292 does just the opposite.

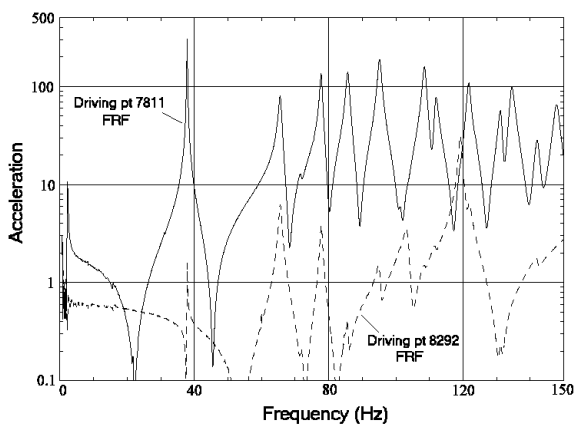

Figure 10. Driving Point Frequency Response Functions for Two Flatwise Inputs.

Extraction of modal frequencies and shapes

Using the measured FRFs for the flatwise input locations, the time domain polyreference technique[9] was used to extract the modal frequencies, dampings, and mode shapes. Because the edgewise bending mode was of special interest, a supplementary test was performed to capture this mode. An instrumented impact hammer was used instead of shakers for the edgewise excitation. The edgewise bending frequency was found at 155.8 Hz, somewhat higher than the modes measured using the flatwise excitation. A total of twelve flatwise modes and the one edgewise mode were extracted from the FRFs. The analysis had actually predicted thirteen flatwise modes below 150 Hz. However, in spite of using the model to determine the excitation locations, only twelve modes were observable in the test data. Of course, the preliminary model can not be expected to be a perfect tool for test design. However, the model was sufficiently accurate and there was more than enough information in the thirteen observed modes to update the FE model.

The measured modal frequencies along with their "interim" model counterparts are shown in the first few columns of Table 2 along with percentage differences between measurement and analysis. Notice that the two sets of frequencies do not align one-to-one. The correspondence between the two sets of modes was obtained visually from the mode shape plots (see Figures 6, 7, 11, and 12) with guidance from the MACs where needed.

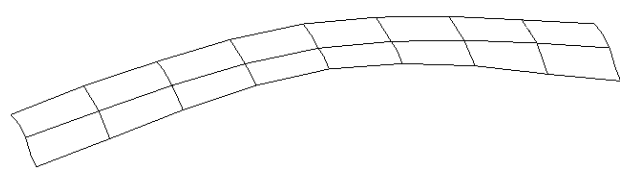

Figure 11: Test-based Mode shape for the First Mode, Flatwise Bending.

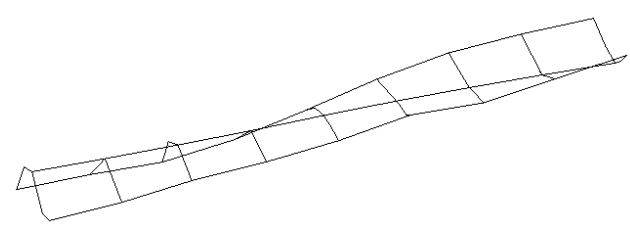

Figure 12: Test-Based Mode shape for the Seventh Mode, Chordwise Bending and Twist.

Mode shapes were also extracted from the FRF data and used to obtain the above mentioned correspondence. Two of the mode shapes are shown in Figures 11 and 12. Figure 11 shows the lowest frequency mode, first flatwise bending, which has the classic shape of the first mode of a free-free beam. Figure 12 reveals a more complicated mode, the

seventh mode called 2nd Chordwise/1st Twist, which contains bending along the chord (chordwise bending), but with twisting. There is one nodal line in the center of the blade span and two lengthwise nodal lines. Using plate terminology, we call this a (1-2) mode shape.

Parameter Estimation

Background

The reconciliation of the computational results from a finite-element analysis with the observations from a modal test requires identifying the parameters within the model that have some uncertainty. These could be material properties, cross-section parameters, densities, joint stiffnesses, or other elements of the model. The test results also have uncertainties, perhaps including proper simulation of the boundary conditions assumed in the analysis, added weight or stiffness due to test fixturing, inaccurately identified modal frequencies, or mode shapes that are not well defined. The reconciliation process then involves reducing the differences between the analysis and the test by adjusting parameters that are believed to be uncertain. The data that is most frequently used for comparison of the test and model are the modal frequencies; these are easily and accurately calculated and relatively easy to measure in the test. Mode-shape data could also be used to augment the modal-frequency data, but that is not typically done because the frequencies provide sufficient information.

Procedure

The parameter estimation was conducted with the aid of a code called PESTDY[4] which has been used for many other parameter estimation efforts at Sandia Labs. Correspondence must be obtained between the analysis mode shapes and the test mode shapes (the modes are often not in the same numerical order) before PESTDY can be applied. This can be done visually, comparing plots of the test and analysis mode shapes. However, it can be difficult in some cases particularly when there are few measurement locations. The MAC matrix, as introduced earlier, is the best procedure for comparing the shapes and obtaining correspondence. This is the motivation for choosing measurement locations to obtain small off-diagonal MACs when the modal test is designed, so that there is little confusion when obtaining correspondence with the analysis shapes.

If there are large differences between test and analysis frequencies for corresponding mode shapes, then the initial estimates for the uncertain parameters need to be adjusted. Since there are typically several parameters to be adjusted and even more frequencies to match, a systematic mathematical approach is required. PESTDY does this by assuming that changes in the calculated frequency can be estimated by multiplying the change in the parameter by the local sensitivity. That is, an updated vector of frequencies f_m is estimated by

$$f_m = \hat{f}_m + S\,\Delta p \quad , \tag{2}$$

where $\hat{f}_m$ is the original model-based vector of frequencies, S is the frequency sensitivity matrix, and Δp is the vector of parameter changes. S is simply the matrix of partial derivatives of the frequencies with respect to the uncertain parameters, so it will normally be a full rectangular matrix. It can be obtained directly from some finite-element codes, but is more commonly obtained by recalculating the frequencies with shifted parameters and estimating the partial derivative with finite differences as was done here.

The PESTDY code solves for the parameter changes Δp that minimize the function below

$$G = (f_m - f_t)^T W_f\,(f_m - f_t) + \Delta p^T W_p \Delta p \,, \tag{3}$$

where f_t is the vector of test frequencies, W_f is the frequency weighting vector, and W_p is the parameter weighting vector. The weights are user-selected factors that allow one to emphasize the parameters and the test frequencies corresponding to the level of confidence, allowing one to account for the uncertainties that might exist in the test data as well as in the parameters. The function G is minimized by setting the gradient of the right hand side of Equation 3 equal to zero and making use of Equation 2. PESTDY then computes the generalized least-squares solution for Δp, the change in parameter values, and the linearly adjusted analysis frequencies, based on Equation 2. The user can interact with PESTDY, iterating on which modes to include, which parameters to vary, and what weights to use. The finite element model is then rerun with the new updated values for the material parameters to determine the new model-based frequencies rather than depending on the linear predictions from PESTDY. If the new frequencies are still too far from the test results, the entire process can be repeated iterativly.

B-Blade Example

The frequency data includes all modes up to 150 Hz, a total of thirteen modes. The first edgewise bending mode was sought out separately and measured at 155.8 Hz. This edgewise mode was included because it strains the cross section differently than the primarily flatwise modes below 150 Hz. A number of PESTDY runs were performed with these data varying the weighting functions and the number of frequencies included to better understand how the process performed. The estimated parameter changes were not sensitive to the selection of weights and the number of frequencies, providing confidence that improved material property estimates were being found. Two of the runs will be discussed here.

Parameter Estimation Results

In the first PESTDY run, all six parameters were assumed to be equally uncertain with small confidence in our initial estimates, so the parameter weights were all set to 0.1. (Normally, the weights are set to be between zero and one.) In contrast, the frequency weights were set higher, varying between 0.4 and 1.0, as we had good confidence in the measured frequencies. The one exception was the 2nd chordwise bending mode which was not excited sufficiently in the test to be identified, so no test frequency was available for that mode, and the frequency weight was set to zero. Table 4 shows the initial analysis frequencies, the test frequencies, and the original errors, then the updated analysis frequencies and the new errors. The last column is explained below.

Table 4 shows that the original errors were reasonably small to begin with, with the exception of the "panel" modes. This good initial correlation is due in part to a previous round of parameter estimation, and is therefore not typical of an initial correlation of model and test data. The PESTDY analysis calculates the material modulus changes required to further improve correlation between analysis and test. Results are shown in Table 3 as the "Final" material property set.

The resulting changes in the model-based frequencies are indicated in Table 4. It is interesting to note that most errors were reduced, but not all of them; so there is a trade-off that the least square algorithm is performing when it attempts to reduce the overall error. As was mentioned above, quite a number of PESTDY analyses were performed using various weights, but the results were not sensitive to weighting choices and the above results are representative of all the analyses.

	Analysis Frequency	**Test Frequency**	**Orig. Error**	**Updated Frequency**	**Updated Error**	**6 Freq. Error**
Mode Number - Name	(Hz)	(Hz)	%	(Hz)	%	%
1 - 1st Flatwise (2-0)	38.1	37.9	+0.6	37.6	-0.7	+0.1
2 - 1st Twist (1-1)	63.8	65.6	-2.6	64.7	-1.3	-1.1
3 - 2nd Flatwise (3-0)	83.0	77.8	+6.7	80.2	+3.1	+0.1
4 - 2nd Twist (2-1)	88.9	85.7	+3.7	86.8	+1.3	-0.5
5 - 1st Chordwise (0-2)	97.2	103.2	-5.8	103.8	+0.6	+2.4
6 - 3rd Panel	104.3	95.1	+9.6	98.7	+3.8	-4.5
7 - 2nd Chord/1st Twist (1-2)	112.4	111.8	+0.5	108.9	-2.6	-6.0
8 - 3rd Twist (3-1)	117.0	119.2	-1.8	112.9	-5.3	-5.3
9 - 2nd Chordwise (0-3)	117.6	-----	----	110.5	-----	-----
10 - 4th Panel/3rd Twist	119.6	108.5	+10.3	114.6	+5.6	+4.2
11 - 4th Twist (2-2)	127.2	131.2	-3.0	123.0	-6.3	-7.7
12 - 5th Panel	132.0	121.7	+8.5	125.7	+3.3	+2.1
13 - 6th Panel	144.2	134.5	+7.2	139.6	+3.7	+3.1
14 - 1st Edgewise	156.6	155.8	+0.5	154.1	-1.0	-0.5
rms of Errors			5.8 %		3.5 %	3.6 %

Table 4: Results from the PESTDY estimation of material properties.

One final analysis was performed to investigate the procedure with fewer modal frequencies. Only six of the measured frequencies were used as input to PESTDY in this analysis. But the effect that the new parameter values would have on the other frequencies were still computed. In this way, some of the measured data is used to update the model, and the other data is used to determine if the model could actually predict frequencies not used in the updating procedure. The six frequencies used were the 1st, 2nd, 4th , 5th, and last (i.e.,

14th) modes,. This analysis produced natural frequency estimates with errors shown in the last column of Table 4, labeled "6 Freq. Error." The new errors are very small and comparable to the errors from the PESTDY analysis which used all the frequency data. This analysis provides additional confidence in the validity of the model in that it can predict modal frequencies *not* used in the updating process. The frequency errors are sufficiently small that it was not necessary to iterate through PESTDY again; however, it is often the case that several iterations are required to converge on an acceptable set of model parameters.

Post Parameter-Estimation Analysis

Using the results from the PESTDY calculations, another modal analysis of the blade was performed. These results are shown in Table 2 along with the experimental values from the modal test and the results from the original parameter estimation. Agreement is good, but not as good as would have been inferred by the linear estimates of the frequency changes from the PESTDY runs.

The changes in blade bending stiffness and torsional rigidity corresponding to the various material properties are shown in Table 5. All analyses were performed using the current model to avoid any differences due to the assumptions made in the interim model. The bending stiffness in both the flatwise and edgewise directions decreased with each modification. This is not surprising since both modifications in material properties decreased the box axial modulus while holding the panel axial value relatively constant (see Table 3). The torsional rigidity increased due to the increase in both the box transverse and shear moduli.

Effective Stiffness	Material Parameters		
	Original	Interim	Final
Flatwise (EI)	1.814	1.639	1.602
Edgewise (EI)	33.19	32.87	32.78
Torsion (GJ)	0.7531	0.7588	0.8093

Table 5: Effective beam stiffness (10^8 lb-in^2) from successive material parameter estimates. All calculations were done using the "current" FE model.

Two nonlinear buckling analyses were also performed using the current model. For both analyses the blade was fixed at one end and a transverse load was applied at the opposite end until buckling occurred. In the first analysis, the interim material parameters were used and the buckling load was 1359 lbs. In the second analysis, the final material parameters were used and the buckling load decreased 10.3% to 1219 lbs. Figure 13 shows overall deformation for the second analysis and Figure 14 shows a closer view of the panel buckling in the tail region. In both cases panel buckling occurred and thus the decrease in the buckling load may be attributed to the decrease in the panel transverse modulus (see Table 3) from 1.871×10^6 psi to 1.424×10^6 psi. The panel axial modulus of 5.027×10^6 psi was identical in both analyses.

Figure 13. Blade fixed at one end with an applied transverse load at the other end. The region near the fixed end is buckling.

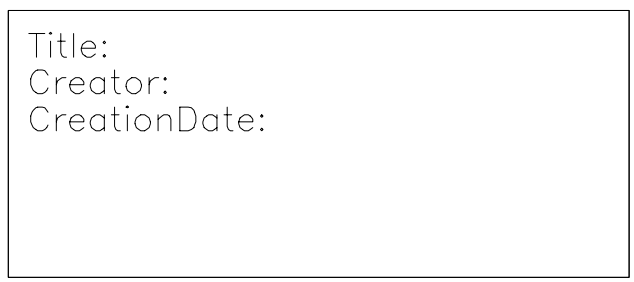

Figure 14. Closer view of buckling region near the fixed end of the blade.

Summary and Conclusions

There are five elements in using parameter estimation to update and improve a finite element model.

1. Initial Modeling and Analysis
2. Test Design
3. Modal Testing
4. Parameter Estimation
5. Model Updating and Analysis

The result is an improved numerical model of the blade that can be used to estimate effective blade properties and to calculate response to loadings that can not be measured. Applications include buckling, detailed stress analysis, and calculating effective beam properties for system dynamics models. In this example of a FloWind blade, updating the material properties resulted in changes to effective beam stiffness measures

by almost 12% and changes to panel-buckling load estimates of about 10%. These changes were for one example only, based on a pultruded blade and a particular composite material system. Therefore, the magnitude of results may not be typical and are by no means the largest effects possible. Additionally, there is always the opportunity for significant modeling error when an FE analysis is attempted. The important point is that this type of parameter estimation procedure can uncover a wide variety of potential modeling errors, improve confidence in model input parameters, and reduce uncertainty in analysis results. The analysis/test combination therefore reduces the risk in fielding a new wind turbine blade design.

References

1. Elliott, A. S., and Wright, A. D., "ADAMS/WT: An Industry-Specific Interactive Modeling Interface for Wind Turbine Analysis," *Wind Energy 1994*, Eds. W. D. Musial, S. M. Hock, and D. E. Berg. SED-Vol. 14. ASME; pp. 111-122, January 1994.
2. Wilson, R. E., Freeman, L. N., Walker, S. N., and Harman, C. R. "FAST Advanced Dynamics Code, Two-bladed Teetered Hub Version 2.4 User's Manual" Final Report: National Renewable Energy Laboratory Golden, CO, March 1996.
3. Garrad Hassan & Partners, The Coach House, Folleigh Lane, Long Ashton, Bristol BS18 9JB, Great Britain.
4. Dohrmann, C. R., "Draft Users Manual for PESTDY", Sandia National Laboratories internal memorandum, April 22,1996.
5. ANSYS, Inc., 201 Johnson Road, Houston, PA 15342-1300, (412) 746-3304.
6. Carne, T. G. and Dohrmann, C. R., "A Modal Test Design Strategy for Model Correlation," Proceedings of the 13th International Modal Analysis Conference, Nashville, TN, Society of Experimental Mechanics, Feb. 13-16, 1995, pp. 927-933.
7. Ewins, D. J., Modal Testing: Theory and Practice, John Wiley & Sons Inc., 1984.
8. Williams, R., Crowley, J., and Vold, H., "The Multivariate Mode Indicator Function in Modal Analysis," Proceedings of the 3rd International Modal Analysis Conference, Society of Experimental Mechanics, 1985.
9. Vold, H., Kundrat, J., Rocklin, G. T., and Russell, R., "A Multi-Input Modal Estimation Algorithm for Mini-Computers," SAE Paper Number 820194, 1982.